[1]Hang Lu
[2]Yubo Shen
[3]Fei Jing
[4]Meng Zhou
[5]Jian Zhang
[6]Hongchen Liu
[7]Chen Zuo

Accurate State Estimation of Lithium-Ion Batteries via a Fractional-Order Model: Synergistic Integration of Snake Optimizer and Fractional-Order Unscented Kalman Filter

Journal of Electrical Systems

Abstract: - Against the backdrop of worsening traditional energy challenges, the automotive industry is shifting from gaso-line/diesel vehicles to new energy alternatives, with lithium-ion battery electric vehicles taking center stage. Accu-rate state of charge (SOC) estimation is critical for battery management systems, relying on precise battery model-ing. This study aims to develop a high-precision framework for battery modeling and SOC estimation in electric vehicles. To accurately simulate battery behavior across frequency bands, an equivalent circuit model integrated with fractional calculus is used instead of traditional capacitors with integer-order capacitors. For precise parame-ter identification, the Snake Optimization (SO) algorithm is employed based on the model's characteristics. Com-pared with the integer-order counterparts, the advantage of fractional-order model is verified. SOC estimation uses the Fractional-Order Unscented Kalman Filter (FOUKF), with the SO algorithm optimizing the filter matrix's initial values to enhance estimation. Experimental results show the optimized strategy significantly improves SOC accu-racy, with maximum error ⩽ 1.5% and convergence error ⩽0.5%, confirming the practicality of the proposed frac-tional-order circuit model and SO-FOUKF algorithm.

Keywords: equivalent circuit model; fractional calculus; snake optimization algorithm; unscented Kalman filter

I. INTRODUCTION

Under the current background of carbon neutrality, traditional fuel vehicles (diesel and gasoline) are clearly no longer aligned with the global development concept, and new energy vehicles have received widespread atten-tion[1-3]. At present, the energy storage components widely used in the industry mainly include three categories: batteries, supercapacitors and high-speed flywheels. These components play a vital role in providing stable energy support, fast charging and long-lasting endurance. However, the most commonly used in new energy vehicles is the power battery with high energy density. Compared with other types of power batteries, lithium-ion power batteries [4-6] have excellent working performance, such as high safety, high energy density, low self-discharge rate, strong temperature adaptability, long service life and stable working voltage range. To ensure the safe and stable operation of lithium batteries, it is essential to monitor their current status in real time. Therefore, the refined modeling and state estimation of lithium-ion batteries have important research significance[7].

The accuracy of a model in fitting battery characteristics significantly influences the representation of both static and dynamic features of the battery[8]. The construction of the battery model is not only deeply restricted by its intrinsic properties, such as electrode materials, but also by many external environmental interferences, for in-stance temperature and the number of working cycles[9] . Due to its complexity, it is extremely difficult to accu-rately build a comprehensive model that can fully describe all battery parameters[10]. The existing battery models can be systematically categorized into three main types: electrochemical models, data-driven models, and equiva-lent circuit models. Because the chemical reaction process of lithium battery is complex, the change of operating state in practice makes it difficult for the electrochemical model to accurately describe the reaction process. As a result, the electrochemical model has not been widely used. The data-driven model relies on a huge amount of ex-perimental data to train the model, and obtains a nonlinear mapping model with superior input-output perfor-mance, such as a neural network model[11-13]. However, the key to data-driven models is to obtain suitable training data, and the model cannot be transferred well. The equivalent circuit model effectively captures the dynamic characteristics of the battery[14-15], depicting it as a combination of electrical components such as resistors and capacitors. All parts of this model have clear physical content and take external environmental factors into account. At the same time, the model has good accuracy and is widely used in engineering practice problems[16].

[2] *Corresponding author: Yubo Shen, State Grid Heilongjiang Electric Power Co., Ltd. Electric Power Science Research Institute
[1,2,3,4,5] State Grid Heilongjiang Electric Power Co., Ltd. Electric Power Science Research Institute
[6,7] School of Electrical Engineering and Automation，Harbin Institute of Technology

The current mainstream equivalent circuit model is integer order, but this model only involves memory information fragments at the current time. Fractional calculus, as an extension of integer calculus, can integrate all information from the past to the present. Therefore, fractional calculus can clearly describe the characteristics of the physical system and can remember and track the changes of the system. Extending the integer calculus elements in the equivalent circuit model to fractional order can enable the model to better reflect the characteristics of the batteries.

At present, the state estimation methods of batteries are mainly concentrated on two types of filter state observers, but due to the complex convergence criteria of the observer, it is very difficult to design an effective state observer. Among the filtering methods, the Kalman series of filters have obvious advantages and can achieve higher calculation accuracy with lower computational complexity. Kalman is based on the optimal data processing method. The algorithm can filter interference noise while obtaining dynamic target data, and then estimate the past, present and future of the target, and can perform smooth interpolation, filtering and prediction functions. The standard Kalman filter only performs well when facing linear systems. Extended Kalman filters (EKF) are an upgrade of KF. The EKF is based on the Taylor series expansion of nonlinear state space equations. It only retains the first-order terms of differentials and ignores higher-order terms, thereby approximating nonlinear systems to linear systems. Although EKF has certain advantages over KF, its disadvantages are also obvious: when the system is converted from linear to nonlinear, the theory of Taylor series expansion is used. This method can only work well when the system maintains continuity and has a high degree of linearization. The prediction results are closely related to process noise and observation noise. If the covariance matrix of the two noises is not accurately estimated, it may cause the accumulation of errors, resulting in a large deviation in the final prediction results, which in turn leads to the divergence of the estimated results.

To solve the above problems, this study uses unscented Kalman filtering for processing. UKF uses unscented transformation to process the system matrix, avoiding the link in EKF where the Jacobian matrix must be calculated, thereby significantly reducing the complexity of the calculation and improving the accuracy of the calculation. At the same time, in order to solve the difficulty in determining the optimal initial value of the error covariance matrix, the strategy of joint improved particle swarm algorithm is adopted to optimize, further improving the ability of Kalman filtering to handle nonlinear dynamic processes. The contributions of this paper can be summarized as fol-lows: a lithium battery equivalent circuit model combined with fractional calculus theory is proposed, and the model parameters are identified; the fractional equivalent circuit model is combined with UKF, and the improved particle swarm algorithm is used to accurately estimate the system state and noise variance to solve the model dif-ference and measurement uncertainty, thus achieving accurate SOC estimation[17-20]. Experiments show that the SOFOUKF(Snake Optimization-Fractional-Order Unscented Kalman Filter) adopted in this paper has excellent performance, can converge quickly and accurately, and can keep the error of SOC estimation after convergence be-low 0.5% in challenging scenarios, and the maximum error during the convergence process does not exceed 1.5%.

The proposed work's novelty and significant contributions are succinctly summarized below.

(1) The equivalent circuit model of fractional calculus is used to describe the battery behavior across frequency bands.

(2) According to the characteristics of fractional-order model, SO algorithm is used to realize the accurate identification of parameters.

(3) Fractional-order unscented Kalman filter is used to estimate SOC, and SO algorithm is applied to optimize the initial value of FOUKF.

The structure of this paper is as follows: Section 2 conducts a comprehensive mathematical analysis of SOC estimation, fractional calculus theory and equivalent circuit model; Section 3 introduces and analyzes the experimental environment and experimental process in detail. Finally, Section 4 gives a conclusion.

II. FRACTIONAL-ORDER EQUIVALENT MODEL OF LITHIUM BATTERY

A. Definition of lithium battery SOC

SOC is one of the key parameters of lithium batteries. There are many different definitions. Although the basic idea is the same, scholars have proposed many definitions from different perspectives such as battery power and energy. The ratio of the remaining battery capacity to the nominal capacity of the lithium battery is the most common measurement method at the same discharge rate. The specific explanation is as follows.

$$\mathrm{SOC}=\frac{Q_C}{Q_I} \tag{1}$$

If the battery is fully charged, SOC = 100%, then:

$$\mathrm{SOC}=(1-\frac{\Delta Q_C}{\Delta Q_I})\times 100\% \tag{2}$$

Where Q_C is the remaining power of the battery, Q_I is the rated capacity of the battery, and ΔQ=0 is the power that has been discharged. The most commonly used method for calculating SOC is the AH integration method. The AH integration method requires the SOC value of the battery at the initial time t_0 to be known. SOC is defined as the sum of the initial soc state and the integral of the battery charge and discharge charge. The calculation formula is:

$$SOC(\mathrm{t})=SOC(t_0)+\frac{1}{Q_0}\int_{t_0}^{t} i_t dt \tag{3}$$

Among them, i_t is the current value during the charging and discharging process of the lithium battery. When charging, i_t takes a positive value, and when discharging, i_t takes a negative value. Q_0 is the actual capacity of the lithium battery. It should be noted that this calculation formula lacks real-time feedback, and its result will be affected by the accumulation of current measurement errors. At the same time, actual factors such as battery degradation, temperature and self-discharge will affect the accuracy of the battery.

B. Definition of Fractional Calculus

Fractional Order Calculus (FOC) is an ancient discipline with a history of several hundred years. It first appeared in Leibniz's diary. As a generalized form of integer order calculus, fractional order calculus is unique in that it can integrate all information from the past to the present, while traditional integer order calculus only involves information fragments at the current moment. Therefore, fractional order calculus can clearly describe the characteristics of the physical system and can remember and track the changes of the system, which is its great advantage over integer order theory[21-24]. As a highly complex physical system, lithium batteries can be well simulated by using fractional calculus theory to describe them.

The fractional calculus operator can be defined as follows:

$$D_{t_0}^{\alpha} f(t)=\begin{cases}\dfrac{d^{\alpha}}{dt^{\alpha}} f(t), \alpha>0\\ f(t), \alpha=0\\ \displaystyle\int_{t_0}^{t} f(\tau)\,d\tau, \alpha<0\end{cases} \tag{4}$$

α is the order of the fractional order, which is a real number; t is the independent variable of the function, t_0 represents the integral's lower limit of integration. When α>0, the operator represents the α-order derivative of the function, with respect to the independent variable, represents the fractional differential t; when α=0 represents the original function, when α<0 represents the negative integral of the original function, the operator expresses the concept of fractional integral. Since the lithium battery fractional system model discussed in this article only involves the application of fractional differentials, and the initial conditions are always set to zero, this part can be ignored.

Fractional calculus is widely used in mathematics and engineering. Because different fields have different research focuses and require different forms of fractional calculus, scholars have proposed multiple definitions of fractional calculus. Among them, the three most common definitions include RL definition, Caputo definition and GL definition. Considering the specific research background and needs of this article, the GL definition is more suitable because of its direct discretization of fractional calculus equations. Therefore, in this study[25], we chose the GL definition as the theoretical basis:

$$D^{\alpha} f(t)=\lim_{T_s\to 0}\frac{1}{T_s^{\alpha}}\sum_{i=0}^{l}(-1)^i\binom{\alpha}{i} f(t-iT_s) \tag{5}$$

In the above formula[26] , T_s represents the sampling time, l represents the duration of memory, and here is l=[(t-t_0)/T_s]. The data point collected in the past [t-t_0, t] time range, which means that the present state is relevant to the past sampling points. $\binom{\alpha}{i}$ represents the Newton binomial coefficient: $\binom{\alpha}{i}=\frac{\alpha!}{(\alpha-i)!i!}$.

C. Establishment of battery equivalent circuit model

Equivalent circuit models are widely used to characterize the dynamic behavior and voltage response of batteries under different current states. The model is constructed by basic circuit elements (voltage source, resistor and capacitor), and usually uses a series RC network to improve accuracy and structural integrity. Taking into account the model accuracy and computational complexity, the first-order model is too simple to accurately describe the circuit behavior of the battery. The computational complexity of the third-order model will be greatly increased. Therefore, the Thevenin equivalent circuit model of the second-order RC network is adopted, as shown in Figure 1 [27].

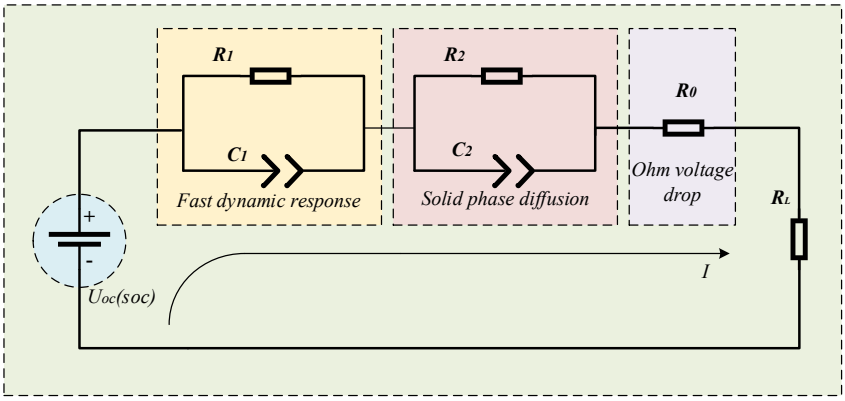

Figure. 1. Fractional-order equivalent circuit model of lithium-ion battery

The circuit model uses a voltage source U_{oc} to accurately characterize the open circuit voltage (OCV) characteristics of the battery. The open circuit voltage characteristics depend on the battery state of charge (SOC), and its identification process is achieved by analyzing the open circuit voltage curve. C_1 and C_2 are capacitor elements with fractional-order characteristics, and R_0, R_1 and R_2 are resistors. R_0 represents the inherent ohmic resistance of the battery, which represents the ohmic voltage drop generated by the battery at the moment of power-on, reflecting the total impedance of the battery electrodes, electrolyte and connecting parts. The parallel links of the two R and fractional-order capacitor elements are used to simulate the polarization effects of the battery on different time scales. The first R_1C_1 branch usually represents the fast dynamic response of the battery electrode process (such as electrochemical double-layer capacitance), and the second R_2C_2 branch represents slower processes such as solid phase diffusion. R_L represents the load resistor, the voltage across it is U_0, and I represents the charge and discharge current.

The circuit can be represented mathematically as:

$$\begin{cases} U = U_{oc} - U_0 - U_1 - U_2 \\ I = C_1 D^{\alpha} U_1 + \dfrac{U_1}{R_1} = C_2 D^{\alpha} U_2 + \dfrac{U_2}{R_2} \end{cases} \tag{6}$$

$$SOC = SOC_0 - \frac{1}{Q}\int_{t_0}^{t} I(t)\,dt \tag{7}$$

According to the principles of fractional calculus theory, the following battery state space equation is established:

$$\begin{cases} \Delta^n x = Ax + BI \\ y = Cx + DI \end{cases} \tag{8}$$

In the above definition, x=[U_1 U_2 SOC]T is the variable of the state space equation; I is the terminal current value of the battery; y is the observed quantity of the system, i.e. , y=[U_0-U_{oc}] is the voltage output by the model, n is the order of the fractional-order system , A,B,C,D is the coefficient matrix:

$$A=\begin{bmatrix} -\frac{1}{R_1C_1} & & \\ & -\frac{1}{R_2C_2} & \\ & & 0 \end{bmatrix}, B=\begin{bmatrix} \frac{1}{C_1} \\ \frac{1}{C_2} \\ -\frac{1}{Q_n} \end{bmatrix}, C=\begin{bmatrix} -1 & -1 & 0 \end{bmatrix}, D=\begin{bmatrix} -R_0 \end{bmatrix} \tag{9}$$

Discretizing the above state equation, the results are as follows:

$$\begin{cases} \Delta^n x_{k+1} = A_k x_k + B_K I_k + w_k \\ y_k = C_k x_k + D_k I_k + v_k \end{cases} \tag{10}$$

According to the GL definition, it is easy to get the following formula:

$$\Delta^n x_{k+1} = \frac{1}{T_s^n} T_s^n \left[x_{k+1} + \sum_{i=1}^{k+1} (-1)^i \binom{n}{i} x_{k+1-i} \right] \tag{11}$$

In the above formula, Ts is the sampling time of the system, take Ts=1, and get the discretization equation of the system:

$$\begin{cases} x_{k+1} = A_k x_k + B_k I_k + w_k - \sum_{i=1}^{k+1} (-1)^i \gamma_i x_{k+1-i} \\ y_k = C_k x_k + D_k I_k + v_k \end{cases} \tag{12}$$

γ_i defined as follows:

$$\gamma_i = \mathrm{diag}\left[\binom{1}{i} \binom{n_1}{i} \right], \binom{n}{i} = \begin{cases} 1, i = 0 \\ \frac{n(n-1)\ldots(n-i+1)}{i!}, \quad i > 0 \end{cases} \tag{13}$$

D. OCV-SOC curve fitting

The hysteresis effect of the battery reveals that the quantity of electricity discharged does not precisely equal the quantity charged. This phenomenon is depicted in the image as two non-overlapping OCV-SOC curves. In order to obtain more precise voltage data, this study employs the average OCV during the charging and discharging processes. This is then used to construct the OCV-SOC curve. The drawn OCV-SOC fitting curve is displayed in Figure 2[29].

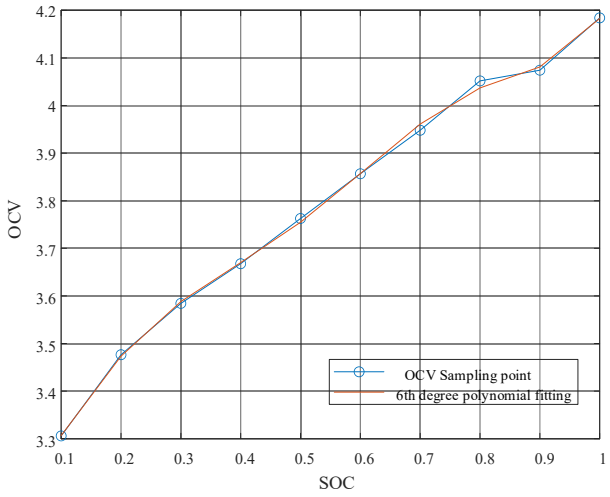

Figure. 2. SOC-OCV Curve Fitting

The experiment found that the fitting performance of the sixth-order polynomial is better than that of the fourth-order and fifth-order polynomials. At the same time, if a higher-order polynomial is used, the function will be very complicated and the improvement in accuracy is not obvious[30]. Therefore, this study uses a sixth-order polynomial for fitting, and its fitting formula is:

$$f(x) = ax^6 + bx^5 + cx^4 + dx^3 + ex^2 + fx + g \tag{14}$$

It is easy to find that a=35.6181, b=-104.5178, c=113.2984, d=-54.5189, e=10.1016, f=1.0577,g=3.1439.

III. PARAMETER IDENTIFICATION AND SOC ESTIMATION OF FRACTIONAL-ORDER MODELS

A. Circuit Parameter Identification Based on SO

The SO algorithm is a new meta-heuristic swarm intelligence optimization algorithm proposed in recent years, which is inspired by the behavioral strategies of snakes in different environments. It is a model based on the mating habits of snakes[31]. Snake mating usually occurs in the cooler spring, and food supply is also a key factor at this time. The algorithm aims to reflect the dependence of the mating process on temperature and food supply. Compared with the particle swarm algorithm, the snake optimization algorithm has a dynamic behavior adjustment mechanism, strong adaptive ability in the search process, and stronger global search ability, especially for multimodal functions. The lithium battery is a highly nonlinear strongly coupled system, and there are multiple coupling parameters in the model. The behavior migration mechanism in the So algorithm helps to integrate distributed exploration with local fine search.

The algorithm constructs a mathematical model with two phases: the exploration phase (characterized by the absence of food) and the development phase (characterized by the presence of physical objects). In the development phase, the model further distinguished two modes: fighting and mating.

(1)Exploration phase (no food)

The exploration phase mainly describes environmental factors. In a cold place with no food, the snake will not look for food around it, but will go to where there is food. At this time, the amount of food is less than the temperature (the temperature is normal).

The formula for male individual position is as follows:

$$X_{i,m}(t+1)=X_{\mathrm{R,m}}(t)\pm c_2\cdot A_{\mathrm{m}}\left(\left(X_{\max}-X_{\min}\right)\cdot \mathrm{R}+X_{\min}\right) \tag{15}$$

Where: $X_{\mathrm{i,m}}$ represents the position of the i-th male individual; $X_{\mathrm{R,m}}$ refers to the position of an arbitrary male individual; c_2 is a constant; R represents a random number, ranging between 0 and 1; A_{m} refers to the capability of the male individual to locate food.

The female individual position formula is as follows:

$$X_{i,f}(t+1)=X_{\mathrm{R},f}(t)\pm c_2\cdot A_f\cdot\left(\left(X_{\max}-X_{\min}\right)\cdot \mathrm{R}+X_{\min}\right) \tag{16}$$

Where: $X_{\mathrm{i,f}}$ is the position of the i female individuals; $X_{\mathrm{R,f}}$ refers to the location of a randomly selected female individual; A_{f} refers to the capability of the female individual to locate food.

(2)Development stage (with food)

The amount of food in the development phase must be greater than the temperature (the temperature is normal), which is the opposite of the exploration phase. If the temperature exceeds the normal range, it can be classified as hot, the snake's movement is unidirectional towards the food, and its position is subsequently updated:

$$X_{i,j}(t+1)=X_{\mathrm{food}}\pm c_3\cdot \mathrm{T}\cdot \mathrm{R}\cdot\left(X_{\mathrm{food}}-X_{i,j}(t)\right) \tag{17}$$

Where: $X_{\mathrm{i,j}}$ represents the position of all individuals, encompassing both males and females; X_{food} represents the optimal individual position; c_3 is a constant (c_2 not equal to); T is the temperature at this time. If the current temperature is below the typical temperature range, it can be inferred that the temperature is currently cold. When threatened or courting, the snake will assume either a defensive or an offensive stance. The two modes are randomly generated with equal probability.

(3)Battle Mode

Currently, the male snake's position is being updated:

$$X_{i,m}(t+1)=X_{i,m}(t)+c_3\cdot E_{\mathrm{FM}}\cdot \mathrm{R}\cdot\left(Q\cdot X_{\mathrm{best,f}}-X_{i,m}(t)\right) \tag{18}$$

In the formula: E_{FM} refers to the combative prowess of the male; Q is the amount of food; $X_{\mathrm{best,f}}$ occupies the dominant position within the female snake hierarchy.

The current position update formula for the female snake is as follows:

$$X_{i,t}(t+1)=X_{i,t}(t)+c_3\cdot E_{\mathrm{FF}}\cdot \mathrm{R}\cdot\left(Q\cdot X_{\mathrm{best,m}}-X_{i,t}(t)\right) \tag{19}$$

In the formula: E_{FM} refers to the combative prowess of the male; Q is the amount of food; $X_{\mathrm{best,f}}$ occupies the dominant position within the female snake hierarchy.

The current position update formula for the female snake is as follows:

$$X_{i,t}(t+1)=X_{i,t}(t)+c_3\cdot E_{\mathrm{FF}}\cdot \mathrm{R}\cdot\left(Q\cdot X_{\mathrm{best,m}}-X_{i,t}(t)\right) \tag{20}$$

Where: E_{FF} represents the combative prowess of the female; $X_{\mathrm{best,f}}$ holds the dominant position within the male snake hierarchy.

(4)Mating mode

In this instance, the locations of both male and female snakes are revised in the manner described below:

$$X_{i,m}(t+1)=X_{i,m}(t)+c_3\cdot M_m\cdot \mathrm{R}\cdot\left(Q\cdot X_{i,t}(t)-X_{i,m}(t)\right) \tag{21}$$

$$X_{i,f}(t+1)=X_{i,f}(t)+c_3\cdot M_f\cdot \mathrm{R}\cdot\left(Q\cdot X_{i,m}(t)-X_{i,f}(t)\right) \tag{22}$$

Where: M_{m} and M_{f} are the mating abilities of males and females respectively. If after the eggs hatch, if there are offspring that are better than the worst parent, the offspring will supplant the least fit parent, necessitating the replacement of both male and female individuals. Figure 3 is the pseudo code of the SO algorithm.

Algorithm 1. Snake Optimization Algorithm

Algorithm: Snake Optimization Algorithm

```
Parameter initialization: maximum number of iterations T, population size N, etc.
Population initialization: Split the population into two equal populations
For t=1:T
    For i=1:N/2
Calculate the fitness value of each individual in the population and find the best female and male individuals
Calculate the temperature Temp and the amount of food Q
        Temp = exp(-t/T)  Q = c1 × exp((t-T)/T)
        If Q<0.25?
            Exploration(Formula 15&16)
        else
            If T>0.6?
                Finding Food(Formula 17)
            Else
                If rand <0.6?
                    Complete mating(Formula 20&21)
                else
                    Battle Mode(Formula 18&19)
                    Replace the worst females and males in the population
                End if
            End if
        End if
    End for
End for
Output the optimal value of the optimization result
```

B. SOC estimation based on FOUKF

This study adopts the Unscented Kalman Filter (UKF) for processing. UKF uses unscented transformation to estimate the system matrix, avoiding the step of calculating the Jacobian matrix in the extended Kalman filter algorithm, thereby significantly reducing the complexity of the calculation and improving the accuracy of the calculation.

The number of sampling points in UKF is small (generally defined as Sigma points), and 2n+1 symmetric Sigma system sampling is generally selected. The operation process of the UKF algorithm can be described as follows:

1) Initialize the state vector matrix and the state estimation error covariance matrix

2) Select the error covariance of the sampling point at the previous moment according to the state vector and calculate the weighted value

3) Use the state space equation to calculate the mean and covariance and update the sampling point

4) Use the nonlinear observation equation to update the selected sampling point endpoint

5) Update the Kalman filter coefficients in real time

The definition of Sigma point is:

1) Construct Sigma point

$$\begin{cases} X^0=\bar{X}, i=0 \\ X^i=\bar{X}+\sqrt{(n+\lambda)P}_i, i=1\sim n \\ X^i=\bar{X}-\sqrt{(n+\lambda)P}_i, i=n+1\sim 2n \end{cases} \tag{23}$$

2) Calculate the weight corresponding to Sigma point

$$\begin{cases} W_m^0 = \dfrac{\lambda}{\lambda + n} \\ W_c^0 = \dfrac{\lambda}{\lambda + n} + (1 - \alpha^2 + \beta) \\ W_m^i = W_c^i = \dfrac{\lambda}{2(\lambda + n)}, i = 1 \sim 2n \end{cases} \tag{24}$$

Where P is the covariance matrix of variable X, i is the number of columns, $\lambda = \alpha^2(n+k) - n$; $10^{-4} \le \alpha \le 1$; k is the secondary scale adjustment factor, usually 0; if the state distribution is Gaussian distribution, take $k=n-3$, which should satisfy the matrix $(n+\lambda)P$ is semi-positive definite; m represents the mean of the sampling point; n represents the covariance of the sampling point; $\beta \ge 0$, for Gaussian distribution, when $\beta = 2$ is the optimal solution.

The following is the iterative formula of the FOUKF algorithm:

$$\begin{cases} \Delta^n \hat{x}_{k|k-1} = A_k \hat{x}_{k-1} + B_k u_{k-1} \\ P_{k|k-1} = (A + \gamma_1) P_{k-1} (A + \gamma_1)^T + \sum_{i=2}^{k} \gamma_i P_{k-1} \gamma_i^T \\ L_k = P_{k|k-1} C^T [C_k P_{k|k-1} C_k^T + R_{k-1}]^{-1} \\ \hat{x}_k = \hat{x}_{k|k-1} + L_k \left(y_k - C \hat{x}_{k|k-1} \right) \\ P_k = (I - L_k C_k) P_{k|k-1} n \end{cases} \tag{25}$$

For FOUKF, the accuracy and robustness of its state estimation are highly dependent on multiple key parameters, especially the initial covariance matrix, process noise covariance matrix and observation noise covariance matrix. P_0 affects the convergence speed and initial stability of the filter, Q_0 reflects the uncertainty of the error and system process, and R reflects the sensor accuracy and measurement disturbance level. At present, the initial value of the matrix is usually determined by empirical methods, which can easily lead to poor convergence or filter divergence. Especially in fractional-order systems, the memory effect of the system is enhanced, and the initial value of the matrix is more sensitive to the result. Therefore, it is necessary to use an optimization algorithm to optimize the initial value of the matrix.The algorithm shown in Figure 3 solves this problem.

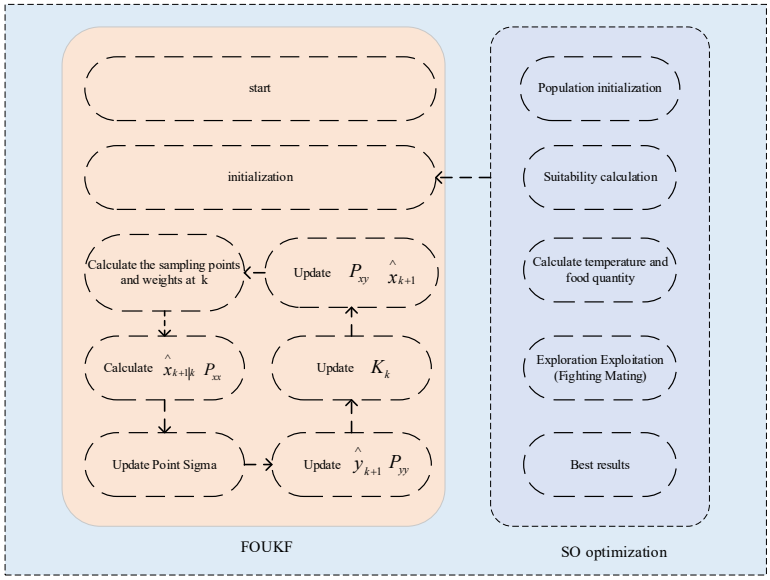

Figure.3. Flowchart of SO-FOUKF

IV. EXPERIMENTAL VERIFICATION

The battery used in this experiment is Yiwei commercial battery, the battery model is INR18650. The experimental environment temperature is room temperature, and the test temperature is 25℃, the specific parameters are as follows:

Table.1 Battery parameters

Item	Data
Model	18650
Rated capacity	3500 mAh
Charge limit voltage	4.20±0.05V
Charge cut-off current	0.02C
Discharge cut-off voltage	2.5V
Operating temperature	25℃

The equipment for testing the external characteristics of the battery is the Xinwei CT-4008T-5V6A-S1 battery charge and discharge detection equipment. The equipment has eight channels, each of which can provide a maximum charge and discharge current of 6A, with a data recording frequency of 10 times per second, a voltage acquisition resolution of 10 mV, a current acquisition resolution of 12mA, a current and voltage sampling accuracy of 0.05%, and a current response time of 1 millisecond. It supports charging modes such as constant current, constant voltage, and constant power charging, and discharge modes such as constant current, constant resistance, and constant power discharge. The hardware system is modularly designed, and the test channels are completely independent and do not interfere with each other. Each channel can be independently programmed and tested, and multiple unit modules can be connected into any combination through serial communication. The equipment communication is based on the TCP/IP network protocol and uses the C/S mode for communication. It can realize the monitoring of thousands of channels by one server, including a data processing system to ensure that data will not be lost due to external reasons during the test. The equipment also has a battery protection function to limit battery overvoltage and overcurrent, thereby improving the safety of the test.

The lithium-ion battery test system consists of a host computer, a middle computer and a battery test device. It adopts a cascade structure and designs the battery test scheme for each channel through the dedicated programming software BTS. The middle computer encodes and transmits data through the connection with the upper and lower computers through the TCP/IP protocol. The battery test device performs corresponding tests on the battery and records the terminal voltage, working current, charge and discharge capacity and other data of the lithium-ion battery in real time, and sends it to the host computer through the middle computer. It can be saved as an EXCEL file to facilitate user data processing. The experimental system is shown in Figure 4.

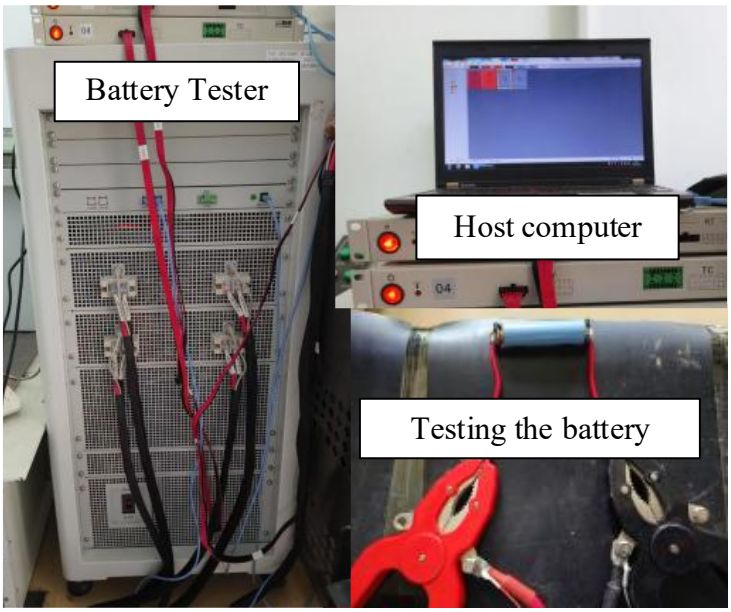

Figure.4. Schematic diagram of experimental test system

In our research, we utilize the Snake Optimization (SO) technique to accurately determine the coefficients of the system model. Throughout the determination process, the order of the model is considered a variable. The model's order is assessed based on the root mean square error (RMSE) between the predicted terminal voltage and the measured terminal voltage . Among them[28]:

$$min: f = \sqrt{\frac{1}{N}\sum_{k=1}^{N}\left(U_k - vol_k\right)^2} \tag{26}$$

Among them, N is the sampling number, U_k represents the terminal voltage estimated by the model, and v_{olk} is the actual voltage. The fitness value change curves are shown in Figure 5 and 6.

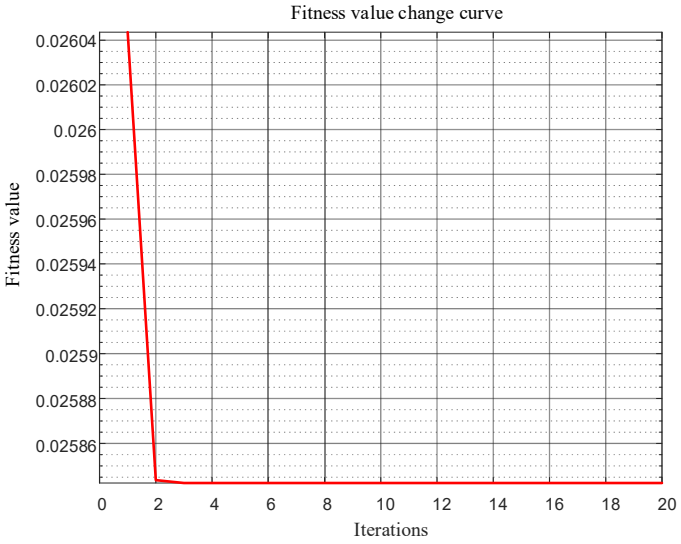

Figure.5. Fitness value curve-Integer order model

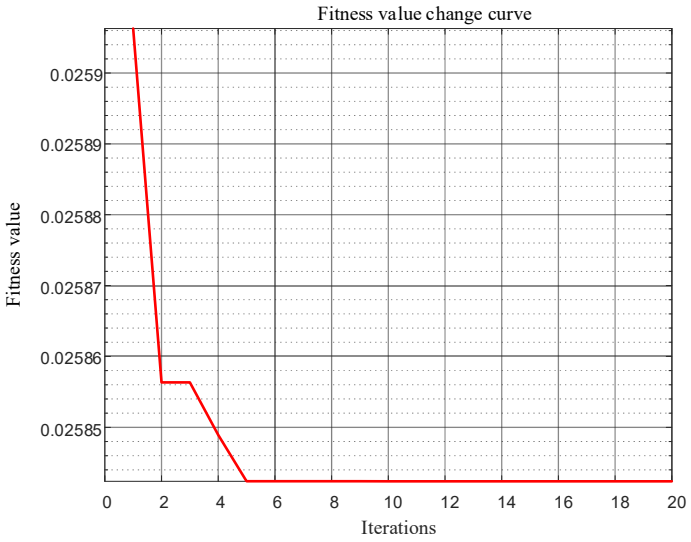

Figure.6. Fitness value curve- Fractional order model

The data used for parameter identification is battery test data under DST conditions at 25°C, and the data used for model verification are FUDS condition battery test data at the same temperature. To ascertain the efficacy of the fractional order model, an analysis and com-parison is conducted on the integer order model.

Table 2. Parameter identification results of Fraction-order

Parameters	Values
R_0/Ω	0.06923
R_1/Ω	0.38735
C_1/F	2807651004.6397
R_2/Ω	0.06423
C_2/F	1068436368.3503
α	0.762399
β	0.749957

Table 3. Parameter identification results of Integer-order

Parameters	Values
R_0/Ω	0.06922
R_1/Ω	0.05282
C_1/F	4530311182.6886
R_2/Ω	0.07325

C_2/F	4855157971.4149

In order to evaluate the actual application of the two models, the two battery models were verified under FUDS conditions, and the model output was compared with the actual value. The results are shown in Figure 7 and Figure 8, where the blue curve is the actual voltage value and the red curve is the model output value. The average error of the integer order model is 0.024252 V and the root mean square error is 0.028425 V. In contrast, the average error of the fractional order model is 0.021232 V and the root mean square error is 0.027413 V. From these results, it can be seen that the fractional order model has higher accuracy than the integer order model, indicating that it is more suitable for use in actual battery management systems.

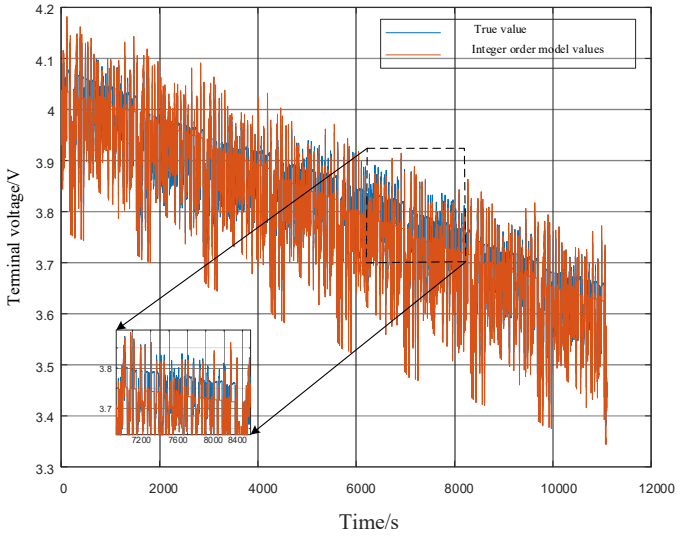

Figure.7. Integer-order model terminal voltage

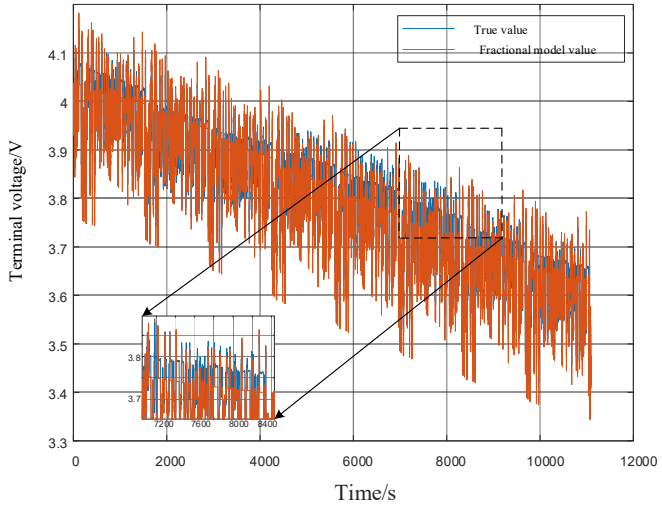

Figure.8. Fractional order model terminal voltage

For the effectiveness of the battery state estimation algorithm, the battery test data under DST conditions is used, the ambient temperature is still 25°C, the model parameters are the same as the previous step, and the model output is compared with the actual output value to verify its accuracy. The terminal voltage and state of charge estimation results under the SO-FOUKF algorithm are shown in Figures 9-12. In Figure 9, the black curve is the true value of the terminal voltage, the red curve is the model output value, the curve in Figure 10 represents the error between the true value of the terminal voltage and the model output value, the black curve in Figure 11 is the true value of the state of charge, the red curve is the model output value of the state of charge, and the curve in Figure 12 represents the error between the actual state of charge value and the model output value.

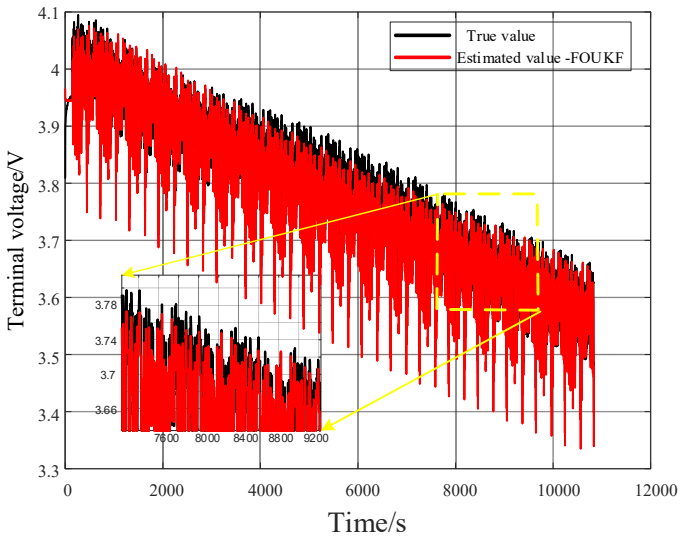

Figure. 9. Terminal voltage estimation

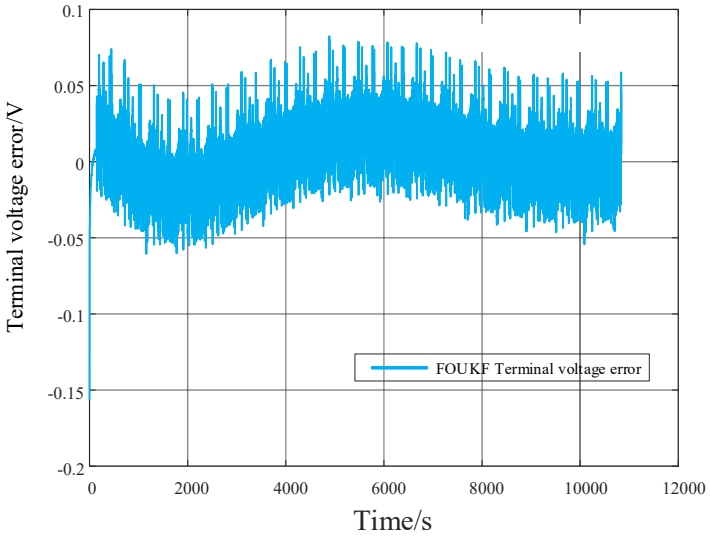

Figure. 10. Terminal voltage estimation error

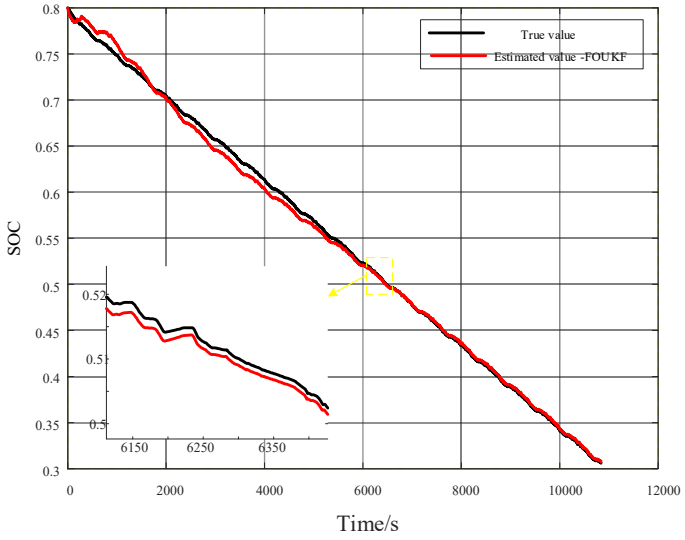

Figure. 12. SOC estimation

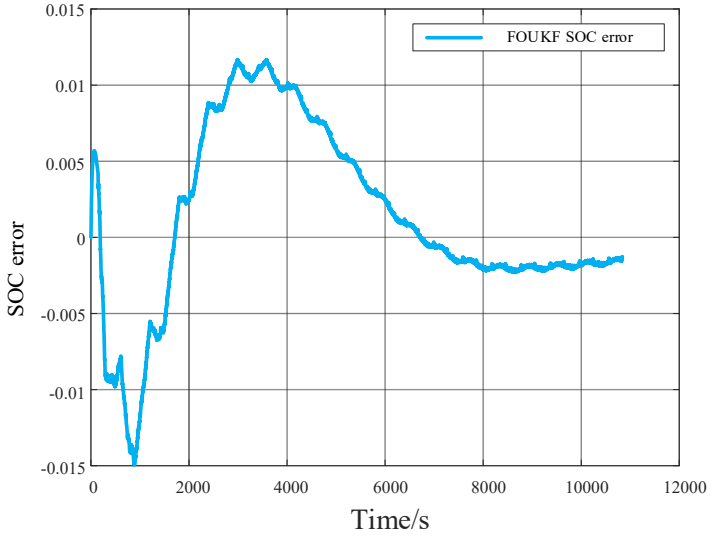

Figure. 13. SOC estimation error

The SOC estimation results based on the SO-FOUKF algorithm are illustrated in the corresponding figures. As shown in Figure 9, the algorithm demonstrates high accuracy in terminal voltage estimation, exhibiting rapid response and effective tracking of the actual voltage signal. According to Figure 10, the absolute voltage estimation error is predominantly within ±0.05 V, with the maximum deviation not exceeding 0.1 V, corresponding to a relative error below 2%. This indicates the algorithm's reliable performance in voltage estimation.

Figure 11 presents the dynamic behavior of SOC estimation. A slight fluctuation is observed during the initial phase; however, the filter quickly converges to the true value and remains stable across the entire SOC range. This demonstrates the algorithm's robustness and applicability throughout the full SOC domain. As shown in Figure 12, the maximum SOC estimation error does not exceed 1.5%, and the final steady-state error is maintained within 0.5%, meeting the requirements for high-accuracy SOC estimation.

In summary, the SO-FOUKF algorithm, when applied to the proposed battery equivalent model, exhibits excellent estimation performance. It proves to be practical for real-world applications, enabling accurate and reliable SOC monitoring and control in battery management systems.

V. CONCLUSION

This study uses a high-order fractional equivalent circuit model to study lithium batteries. Through theoretical analysis, the state space expression of the second-order fractional circuit model is derived, mainly including terminal voltage and state of charge. The model parameters are accurately identified using the SO algorithm and curve fitting, and the accuracy is verified using different working conditions. The accuracy of the developed parameter identification method exceeds 98%. In order to achieve accurate state estimation of lithium-ion battery SOC, fractional-order unscented Kalman filter and SO algorithm are combined. The fractional-order unscented Kalman filter solves the problem that the traditional extended Kalman filter has large errors for nonlinear systems. The SO algorithm is used to optimize the initial value of the matrix to improve the filtering effect. The experiment verifies the effectiveness of the algorithm, and the error margin is less than 2%. Although this study has conducted a relatively comprehensive study on battery management and state of charge estimation, there are still some problems: lithium batteries are extremely susceptible to temperature and material aging, which will significantly reduce the applicability of the algorithm. This reminds us of the future research direction and proposes a more comprehensive strategy to deal with these problems.

ACKNOWLEDGMENT

This work was supported by the Science and Technology Project of State Grid Heilongjiang Electric Power Co., Ltd. (Research on Health State Estimation and Life Prediction Technology for Lithium-ion Batteries in Battery Energy Storage Power Stations) under Grant SGHLDKO0PJJS2400081.

REFERENCES

[1] Xiong, R., Sun, X., Yang, R., Shen, W., He, H., & Sun, F. Sensors-enabled approach for real-time quantification of lithium plating under extreme environments. Applied Energy, 2025,397, 126370.

[2] Wang, L., Zhang, P., Guo, Z., Wang, J., Ma, J., & Ji, Z. Y. Electrochemical lithium extraction by the faradaic materials: advances, challenges and enhancement approaches. Acta Physico-Chimica Sinica, 2025, 100127.
[3] Demirci, O., Taskin, S., Schaltz, E., & Demirci, B. A. Review of battery state estimation methods for electric vehicles-Part I: SOC estimation. Journal of energy storage, 2024, 87, 111435.
[4] Xiong, R., Cao, J., Yu, Q., He, H., & Sun, F. Critical review on the battery state of charge estimation methods for electric vehicles. IEEE Access, 2017, 6, 1832-1843.
[5] Lopes, J. A. P., Soares, F. J., Almeida, P. M. R. Integration of electric vehicles in the electric power system. Proceedings of the IEEE. 2010, 99(1), 168-183.
[6] Li, H., Wang, Z., Chen, L., & Huang, X. (2009). Research on advanced materials for Li‐ion batteries. Advanced materials, 2009, 21(45), 4593-4607.
[7] Hu, X., Li, S., Peng, H. A comparative study of equivalent circuit models for Li-ion batteries. Journal of Power Sources. 2012, 198, 359-367.
[8] Horner, J. S., Whang, G., Kolesnichenko, I. V., Lambert, T. N., Dunn, B. S., Roberts, S. A. A pseudo-two-dimensional (P2D) model for FeS2 conversion cathode batteries. Journal of Power Sources. 2022, 544, 231893.
[9] El Fallah, S., Kharbach, J., Hammouch, Z., Rezzouk, A., Jamil, M. O. State of charge estimation of an electric vehicle's battery using Deep Neural Networks: Simulation and experimental results. Journal of Energy Storage. 2023, 62, 106904.
[10] Zhao, X., Cai, Y., Yang, L., Deng, Z., & Qiang, J. State of charge estimation based on a new dual-polarization-resistance model for electric vehicles. Energy. 2017, 135, 40-52.
[11] Chen, D., Xiao, L., Yan, W., Guo, Y. A novel hybrid equivalent circuit model for lithium-ion battery considering nonlinear capacity effects. Energy Reports. 2021, 7, 320-329.
[12] Zou, C., Manzie, C., Nešić, D. A framework for simplification of PDE-based lithium-ion battery models. IEEE Transactions on Control Systems Technology. 2015, 24(5), 1594-1609.
[13] Pande, A. S., Sharma, A. K., & Soni, B. P. State of Charge Estimation Using Extended Kalman Filter for Li-Ion Battery With Its Internal Parameter. In Modern Computing Technologies for EV Efficiency and Sustainable Energy Integration, 2025, (pp. 221-250). IGI Global Scientific Publishing.
[14] Khalil, M., Postoyan, R., & Raël, S. Systematic Observer Design With Robust Global Convergence Guarantees for a Large Class of Lithium-Ion Battery Models, 2025, IEEE Control Systems Letters.
[15] Huang, B., Li, H., Sun, J., Sun, J., Tian, X., Song, K., ... & Wang, Z. Robust SOC estimation for lithium-ion batteries: Combination of GRU and FOMIAUKF approach with an improved state transition matrix. Energy, 2025, 136429.
[16] Waag, W., Käbitz, S., Sauer, D. U. Application-Specific Parameterization of Reduced Order Equivalent Circuit Battery Models for Improved Accuracy At Dynamic Load. Measurement. 2013, 46(10), 4085-4093.
[17] Gao, L., Liu, S., Dougal, R. A. Dynamic Lithium-Ion Battery Model for System Simulation. IEEE transactions on components and packaging technologies. 2002, 25(3), 495-505.
[18] Wang, S., Huang, P., Lian, C., & Liu, H. Multi-interest adaptive unscented Kalman filter based on improved matrix decomposition methods for lithium-ion battery state of charge estimation. Journal of Power Sources, 2024, 606, 234547.
[19] Jiang, B., Zhu, J., Wang, X., Wei, X., Shang, W., Dai, H. A Comparative Study of Different Features Extracted from Electrochemical Impedance Spectroscopy in State of Health Estimation for Lithium-Ion Batteries. Applied Energy. 2022, 322, 119502.
[20] Chen, Y., Yang, X., Luo, D., Wen, R. Remaining Available Energy Prediction for Lithium-Ion Batteries Considering Electrothermal Effect and Energy Conversion Efficiency. Journal of Energy Storage. 2021, 40, 102728.
[21] Diethelm, K., Ford, N. J. Analysis of Fractional Differential Equations. Journal of Mathematical Analysis and Applications. 2002, 265(2), 229-248.
[22] Tepljakov, A., Petlenkov, E., Belikov, J., Petráš, I. FOMCON Toolbox for Modeling, Design and Implementation of Fractional-Order Control Systems. Applications in control. 2019, 6, 211-236.
[23] Soukkou, A., Soukkou, Y., Haddad, S., Lekouaghet, B., & Benghanem, M. Design tools to stabilize and to synchronize fractional-order energy resources system based on fractional-order control approaches: a review. Journal of the Brazilian Society of Mechanical Sciences and Engineering, 2025, 47(4), 173.
[24] Yang, Q., Chen, D., Zhao, T., Chen, Y. Fractional Calculus in Image Processing: A Review. Fractional Calculus and Applied Analysis. 2016, 19(5), 1222-1249.

[25] Wang, B., Li, S. E., Peng, H., Liu, Z. Fractional-order Modeling and Parameter Identification for Lithium-Ion Batteries. Journal of Power Sources. 2015, 293, 151-161.
[26] Zou, C., Zhang, L., Hu, X., Wang, Z., Wik, T., Pecht, M. A Review of Fractional-Order Techniques Applied to Lithium-Ion Batteries, Lead-Acid Batteries, And Supercapacitors. Journal of Power Sources. 2018, 390, 286-296.
[27] Hu, M., Li, Y., Li, S., Fu, C., Qin, D., Li, Z. Lithium-Ion Battery Modeling and Parameter Identification Based on Fractional Theory. Energy. 2018, 165, 153-163.
[28] Zhou, D., Zhang, K., Ravey, A., Gao, F., Miraoui, A. Parameter Sensitivity Analysis for Fractional-Order Modeling of Lithium-Ion Batteries. Energies. 2016, 9(3), 123.
[29] Zou, C., Hu, X., Dey, S., Zhang, L.,Tang, X. Nonlinear Fractional-Order Estimator with Guaranteed Robustness and Stability for Lithium-Ion Batteries. IEEE Transactions on Industrial Electronics. 2017, 65(7), 5951-5961.
[30] Wang, S., Xiao, X., & Ding, Q. A novel fractional system grey prediction model with dynamic delay effect for evaluating the state of health of lithium battery. Energy, 2024, 290, 130057.
[31] Hashim, F. A., Hussien, A. G. Snake Optimizer: A Novel Meta-Heuristic Optimization Algorithm. Knowledge-Based Systems. 2022, 242, 108320.